

Supporting Information for:

## Layer-by-Layer Assembled Multilayers of Polyethylenimine-Stabilized Platinum Nanoparticles and PEDOT:PSS as Anodes for the Methanol Oxidation Reaction

Kyler R. Knowles,<sup>†</sup> Colin C. Hanson,<sup>‡</sup> April Levu Fogel,<sup>†</sup> Brian Warhol<sup>‡</sup> and David A. Rider<sup>‡,†\*</sup>

<sup>†</sup>Department of Engineering Technology, Western Washington University,  
516 High St., Bellingham WA 98225

<sup>‡</sup>Department of Chemistry, Western Washington University,  
516 High St., Bellingham WA 98225

\* To whom correspondence should be addressed: david.rider@wwu.edu

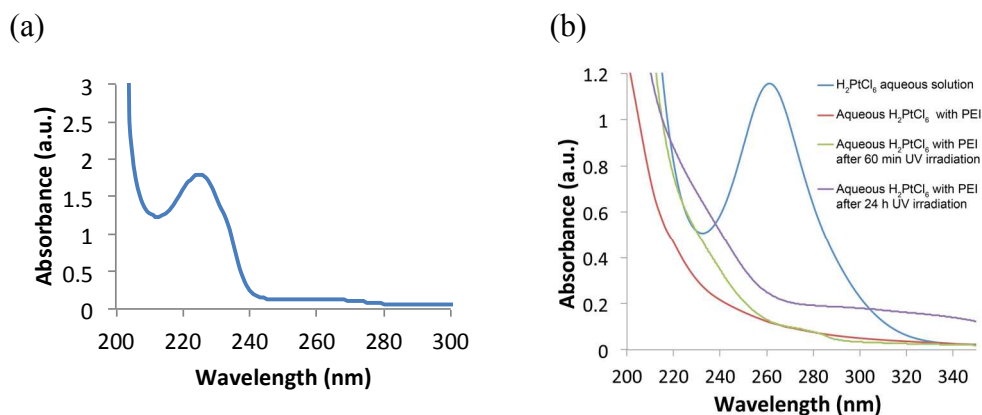


**Figure S1.** UV-Vis spectra characterization of aqueous (a) (PEDOT:PSS)Na<sup>+</sup> and (b) H<sub>2</sub>PtCl<sub>6</sub>, H<sub>2</sub>PtCl<sub>6</sub>-loaded PEI, PEI-capped Pt NPs after 60 min UV photoreduction and PEI-capped Pt NPs after 24 hrs UV photoreduction.

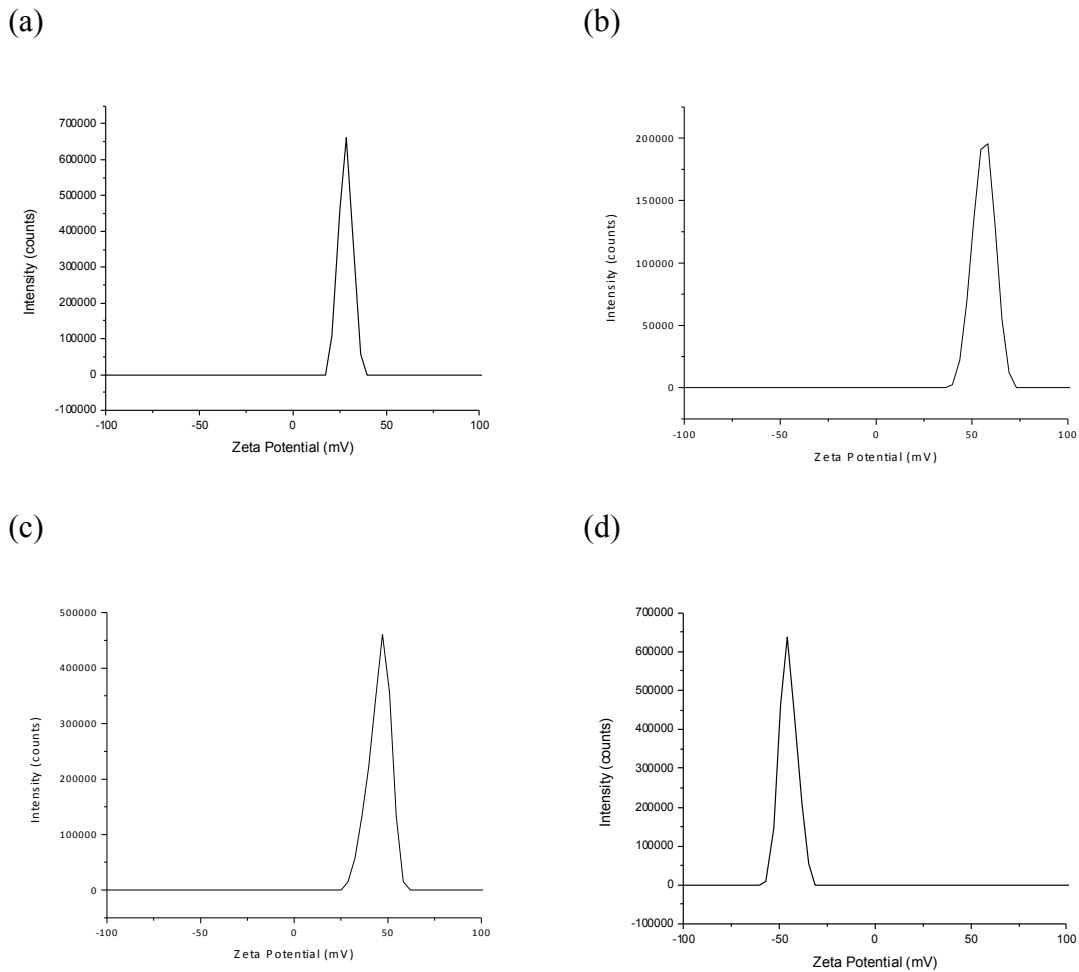


**Figure S2.** Zetapotential traces for (a) PEI, (b) H<sub>2</sub>PtCl<sub>6</sub>-loaded PEI, (c) PEI-capped Pt NPs and (d) (PEDOT:PSS)<sup>-</sup>Na<sup>+</sup>.

To confirm the presence of the Pt NPs and the PEDOT conductive element in the multilayers, a series of films were studied by laser-ablation inductively coupled plasma mass spectroscopy (LA ICP-MS, see Table S1 for experimental parameters). LA ICP-MS was selected for element-specific detection in order to track the abundance of the constituent elements for the NPs and the conducting polymer for a series of [PEI-capped Pt NPs/(PEDOT:PSS)]<sub>n</sub> films within the range  $n=0-20$ . Specifically, the intensity in the signal for <sup>195</sup>Pt and <sup>34</sup>S isotopes was monitored as the bilayer number was varied in an effort to confirm the incorporation of each component into the multilayer films. All other

relevant isotopic signals for elements from the multilayer (i.e. C, N, O) were unfortunately not resolved from inadvertent background contamination levels and could not be tracked in the same manner. Shown in Figure S3a is a summary plot for the signal intensities for  $^{195}\text{Pt}$  and  $^{34}\text{S}$  ions as a function of the bilayer number for the samples. The trends in both elemental signals are reminiscent of those seen in the optical density absorption spectroscopy and film thickness studies. As the bilayer number increases, there is a matched increase in the abundance of Pt and S elements in the coating, which suggests that  $[\text{PEI-capped Pt NPs}/(\text{PEDOT:PSS})]_n$  multilayers are deposited with a uniform composition. Given that the ITO substrate has a thickness of 25 nm and its composition is approximately 90  $\text{In}_2\text{O}_3$ :10 $\text{SnO}_2$ ,<sup>1</sup> the atomic concentration of Pt and S can be determined from the film thickness data in Figure 3d and the Sn signal in the fully ablated ITO substrate. Figure S3b reports the relative concentration of Pt and S in  $[\text{PEI-capped Pt NPs}/(\text{PEDOT:PSS})]_n$  multilayers for  $n=5-20$ . When normalized for the increasing film thickness, the relative atomic concentration of Pt and S in the directly ablated films were found to approach  $\sim 0.07\%$  and  $\sim 0.02\%$ , respectively. For a series of samples resolved at a half-bilayer value, namely multilayers with  $n=10, 10.5, 11, 11.5, 12$  and  $12.5$ , ICP-MS also distinguished multilayers terminated with PEI-capped Pt NPs (see Figure S3c). Similarly, the platinum loading in  $[\text{PEI-capped Pt NPs}/(\text{PEDOT:PSS})]_n$  films can be determined from ICP-MS analysis of nitric acid digested films. Briefly, ITO-supported multilayers of known thickness and area were digested with 1.00 mL of analysis grade nitric acid for 10 hrs followed by dilution with 10.00 mL of ultra-pure water. These solutions were then analyzed for the  $^{195}\text{Pt}$  isotopic signal and converted to Pt concentration using a calibration sample set of known Pt concentration (1 ppm to 1 ppt). Table S2 reports the resulting estimate for Pt-loading per unit volume of multilayer film. As higher bilayer number films are targeted the Pt-loading approaches a value of 1.3  $\text{mg}/\text{cm}^3$ .

**Table S1.** Optimized conditions element specific detection by LA-ICP-MS.

| <b>ICP-MS: Agilent 7500 CE</b> |                                    | <b>LA system: UP213</b>  |                             |
|--------------------------------|------------------------------------|--------------------------|-----------------------------|
| RF Power                       | 1550 W                             | laser energy             | 100% (~3.9 mJ)              |
| Torch gas Flow Rate (Ar)       | 1.22 L min <sup>-1</sup>           | laser frequency          | 10 Hz                       |
|                                |                                    | laser diameter           | 55 μm                       |
| cones                          | Ni skimmer<br>Ni sampler           | ablation mode            | single line scan for 33.7 s |
|                                |                                    | scan speed               | 15 μm s <sup>-1</sup>       |
| isotopes                       | <sup>34</sup> S, <sup>195</sup> Pt | pre-acquisition ablation | 30 s                        |
| sample integration time        | 0.1 s                              | acquisition time         | 3.7 s                       |
|                                |                                    | carrier gas (He)         | 0.6 L min <sup>-1</sup>     |

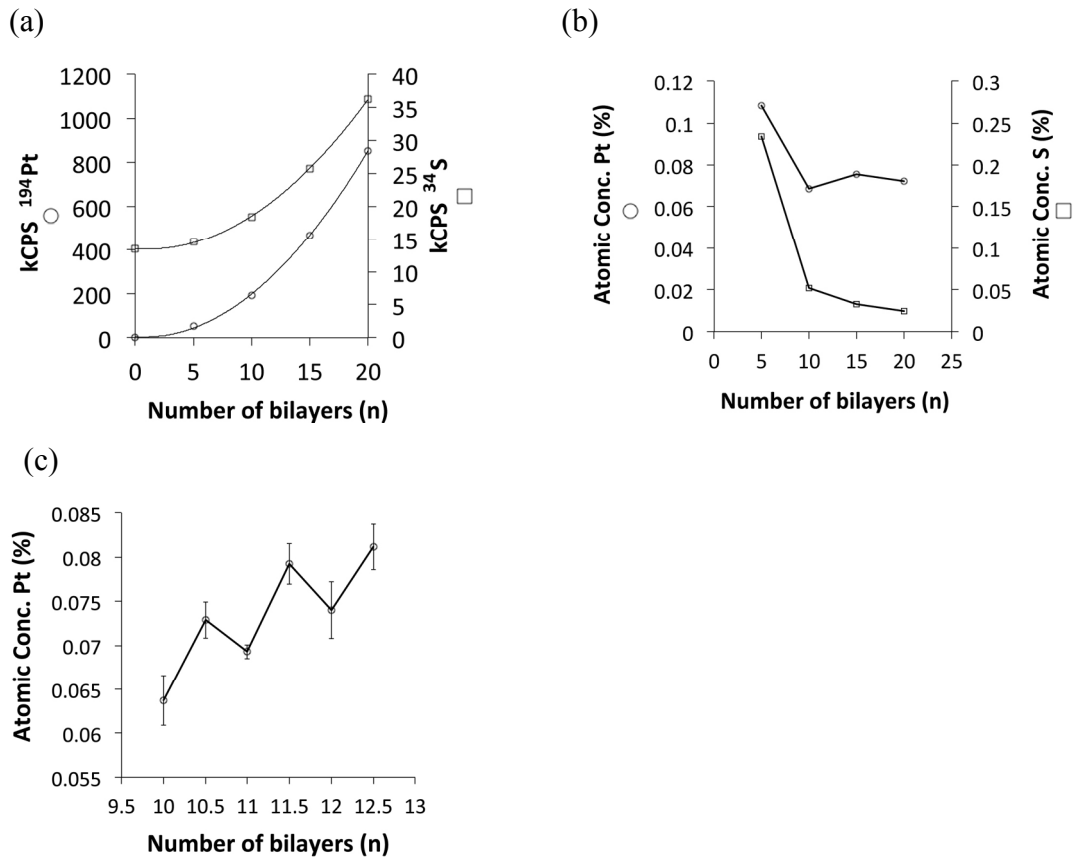


**Figure S3.** (a) LA ICP-MS signal for  $^{195}\text{Pt}$  and  $^{34}\text{S}$  ions in  $[\text{PEI-capped Pt NPs}/(\text{PEDOT:PSS})]_n$  where  $n=0-20$ . (b) Relative atomic concentrations of Pt and S in  $[\text{PEI-capped Pt NPs}/(\text{PEDOT:PSS})]_n$  where  $n=5-20$ . (c) Relative atomic concentration of Pt resolved to the half-bilayer in  $[\text{PEI-capped Pt NPs}/(\text{PEDOT:PSS})]_n$  multilayers for  $n=10-12.5$ .

**Table S2.** Summary of platinum loading in  $[\text{PEI-capped Pt NPs}/(\text{PEDOT:PSS})]_n$  films.

| <u>Number of bilayers (<math>n</math>)</u> | <u>Platinum Loading (<math>\text{mg}/\text{cm}^3</math>)</u> |
|--|--|
| 5  | 21.2   |
| 10   | 3.0  |
| 15   | 1.7  |
| 20   | 1.3  |

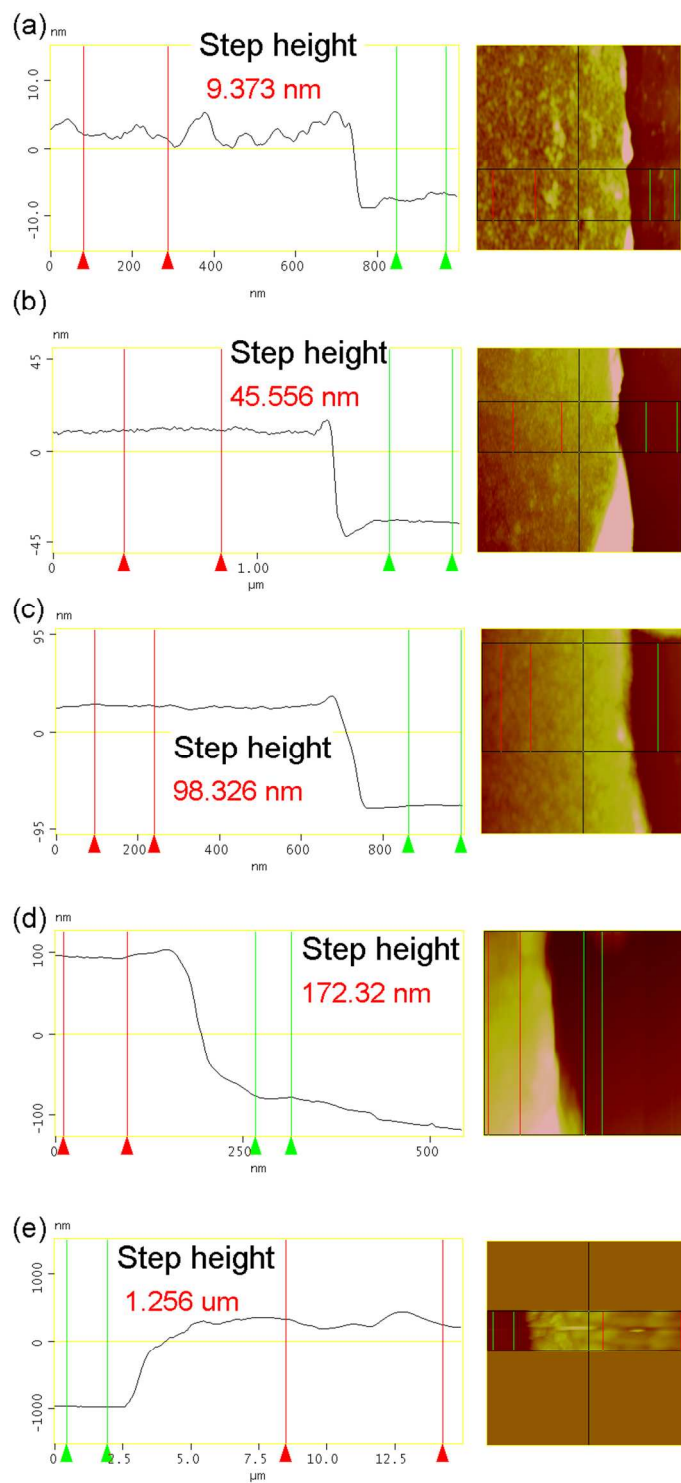


**Figure S4.** SFM step-height analysis of  $[PEI\text{-capped Pt NPs}/(PEDOT:PSS)]_n$  multilayer films on quartz where (a)  $n = 5$  (b)  $n = 10$ , (c)  $n = 15$  (d)  $n = 20$ . (e) SFM step-height analysis of  $[PEI/(PEDOT:PSS)]_{20}$  multilayer film on ITO.

The nanoparticle number density ( $n$ ) can be estimated from the equations for the mass yield from the TGA analysis (eq. 1) and the mass estimate for Pt NPs and the surrounding matrix (eq. 2 and 3 respectively). The input mass densities ( $\rho$ ) for bulk Pt, (PEDOT:PSS) $^-$ Na $^+$  and PEI are 21.5, 1.50 and 1.05 g/cm $^3$ , respectively. For this estimate it is assumed that the mass yield is an additive value determined by the constitute materials and that the mass density of the matrix hosting the Pt NPs has a value between (PEDOT:PSS) $^-$ Na $^+$  and PEI. To estimate the nanoparticle density in [PEI-capped Pt NPs/(PEDOT:PSS)] $_{20}$ , a  $V_{\text{multilayer}}$  defined by 1  $\mu\text{m}$  x 1  $\mu\text{m}$  x 0.172  $\mu\text{m}$  dimensions was used.

$$\text{Mass Yield} = \frac{\text{Mass Pt NPs}}{\text{Mass Pt NPs} + \text{Mass Matrix}} \quad (1)$$

$$\text{Mass Pt NPs} = n \cdot \rho_{\text{Pt}} \cdot \frac{4}{3} \pi r_{\text{Pt NP}}^3 \quad (2)$$

$$\text{Mass Matrix} = \rho_{\text{matrix}} [V_{\text{multilayer}} - (n \cdot \frac{4}{3} \pi r_{\text{Pt NP}}^3)] \quad (3)$$

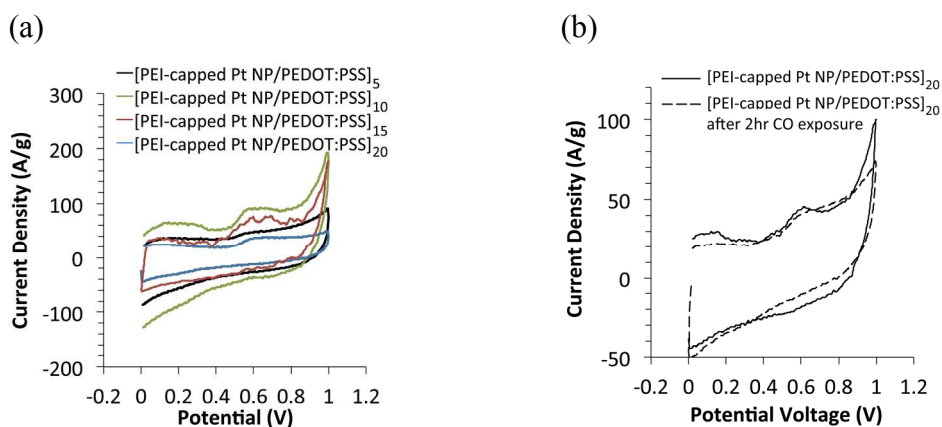


**Figure S5.** (a) Cyclic voltammetry (vs. Ag/AgCl) plots for methanol oxidation reaction catalyzed by a [PEI-capped Pt NPs/(PEDOT:PSS)]<sub>n</sub> multilayer working electrode at 0.050 V/sec in 0.1 M H<sub>2</sub>SO<sub>4</sub> and 2 M CH<sub>3</sub>OH where n=5-20. (b) Cyclic voltammetry (vs. Ag/AgCl) plots for methanol oxidation reaction catalyzed by [PEI-capped Pt NPs/(PEDOT:PSS)]<sub>20</sub> without (—) and after a 2 hr CO exposure (---).

## REFERENCES

1. *Delta Technologies, CG-IN90 Product Information.*